Journal of Water & Health

Journal of Water and Health Vol 19 No 6, 933 doi: 10.2166/wh.2021.113

Assessment of radiation dose hazards caused by radon and its progenies in tap water by the human dosimetric model

Jinlong Yong[a], Qian Liu[b], Baoshan Wu[a], Youhua Hu[c] and Guangwen Feng[a,*]

[a] Research Center of Radiation Ecology and Ion Beam Biotechnology, College of Physics Science and Technology, Xinjiang University, Urumqi, Xinjiang 830046, China
[b] School of Statistics and Data Science, Xinjiang University of Finance & Economics, Urumqi, Xinjiang 830012, China
[c] Radiation Environment Supervision Station of Xinjiang, Urumqi, Xinjiang 830000, China
*Corresponding author. E-mail: fenggw@xju.edu.cn, feng_guang_wen@163.com

ABSTRACT

Radon is readily soluble in water, and radon exposure caused by household water consumption may pose a threat to public health. In this study, the radon concentration in the tap water of residential buildings was measured, and the average value was 543.33 mBq L^{-1}, which was in line with the radon concentration limit recommended by USEPA (11.11 Bq L^{-1}) and EURATOM (100 Bq L^{-1}), and also within the range of the results of radon concentration measurements in tap water in other countries or regions. Through water bath heating at different temperatures, the radon retention curves of multiple groups of samples at different temperatures were fitted and analyzed. The results showed that the radon retention continued to decrease between 25 and 70 °C, remained stable between 70 and 85 °C, and then continued to decline slowly. Combined with the measurement results, the effective doses of α- and β-particles emitted by ^{222}Rn and its progenies to residents respiratory and alimentary tissues and organs were calculated using the computational model provided by ICRP under two typical water scenarios of shower and drinking water, and the results show that radon exposure caused by normal water consumption will not pose a serious threat to public health.

Key words: human dosimetric model, radon concentration, radon retention rate, tap water

HIGHLIGHTS

- The radon concentration of domestic tap water in Urumqi, Xinjiang was measured.
- The variation trend of radon concentration in tap water with temperature was analyzed.
- The radiation dose contributed by radon exposure to residents under different water-use scenarios was calculated based on the actual water temperature.
- The radiation doses to human organs from the α and β decay progenies of radon were calculated.

1. INTRODUCTION

Radon, a colorless, odorless inert radioactive gas, has four radioactive isotopes (^{218}Rn, ^{219}Rn, ^{220}Rn, and ^{222}Rn) in nature. ^{222}Rn has received extensive attention because its parent nucleus ^{226}Ra is abundant in soil and rock and has the longest half-life (3.82 days) (ICRP 2007). The decay of ^{222}Rn emits α-particles and produces a series of short-lived progenies such as ^{218}Po, ^{214}Pb, ^{214}Bi, and ^{214}Po (UNSCEAR 2000). Considering the soluble readily in water, ^{222}Rn can easily diffuse from solid materials into the water and be transported when various types of water resources in nature come into contact with soil and rocks (Zhuo *et al.* 2001; Yasouka *et al.* 2008; Jantsikene *et al.* 2014; Mehra *et al.* 2016).

Water is an important factor affecting public health (WHO 2009). The major source of domestic water for urban residents is tap water supplied through the urban water supply network. ^{222}Rn dissolved in tap water can be transported to residential buildings far away from water supply plants in a short period through the pipe network, and then degassed from water to indoor environment in the process of domestic water use, or be ingested by residents along with drinking water or food (UNSCEAR 2000; Vinson *et al.* 2008). The ^{222}Rn and progenies which enter the respiratory system of the human body through respiration cannot be completely filtered, in breathing, the inhaled ^{222}Rn is almost exhaled again, but the progenies of decay can attach to air particles and have a certain probability in the respiratory tract tissue surface adhesion and deposition (Vinson *et al.* 2008; Oner *et al.* 2009), α- or β-particles emitted by the decay of these short-lived progenies cause genetic damage to the cells on the surface of the deposited organ or tissue and can also penetrate the mucous membrane on the surface of the tissue or organ, causing damage to stem cells deep inside those tissues or organs (Zhuo *et al.* 2001; Kendall & Smith 2002; Darby *et al.* 2005; Alghamdi & Aleissa 2014). Meanwhile, some progenies are transferred to the body fluids through which they are transported to organs other than the respiratory organs, causing radiation damage to those organs. The ingestion of tap water with a higher ^{222}Rn concentration was also associated with an increased risk of visceral disease, especially the incidence of gastric cancer and gastrointestinal cancer. Besides causing radiation damage to surface cells in the lining of digestive organs, ^{222}Rn can also be absorbed by the gastrointestinal tract into body fluids and cause damage to other radiation-sensitive tissues or organs in the body. Therefore, the measurement and dose assessment of ^{222}Rn and its progenies in tap water are of great significance in preventing random biological effects and improving public health (Kulali *et al.* 2019).

Many previous studies have calculated the effective inhaled or ingested dose of radon exposure due to domestic water (Binesh *et al.* 2012; Nita *et al.* 2013; Sharma *et al.* 2019). Nevertheless, the dose calculation of α- and β-particles to specific organs and tissues in the respiratory tract and alimentary tract is rarely involved, and the effect of temperature on radon concentration in water was not considered. In the present study, ^{222}Rn concentrations in different tap water samples were measured, and the variation trend of ^{222}Rn concentrations in tap water at different temperatures was analyzed. Based on the measurement results, the effective doses of α- and β-particles to the public were estimated using the human respiratory and alimentary tract model the human digestive tract model provided by ICRP.

2. MATERIALS AND METHODS

2.1. Sample collection and determination of radon concentration

Urumqi River is the water source of Urumqi City in Xinjiang. The water supply plants in the city carry out centralized filtration and purification treatment for the river water and then transport it to the residents. In the study, 400 mL glass sampling bottles were used to collect indoor tap water from six residential areas in Urumqi. After the collection, the samples were sealed and brought back to the laboratory for radon concentration measurement under a constant temperature environment. Meanwhile, the collected water samples are heated to 25, 40, 55, 70, 85, and 100 °C in a constant temperature water bath with the same water bath time, and the radon concentration in the samples was measured at different water bath temperatures. All the measurements are completed on the same day of sampling.

The concentration of radon in the sample was measured by FD216, an environmental radon measurement instrument based on the scintillation chamber method, and its principle and structure are shown in Figure 1. Detailed experimental methods and procedures are described in the previous work (Yong *et al.* 2020).

2.2. Estimation of radon and its progenies in the air

The transfer coefficient of radon in tap water diffusing into the air is calculated as follows:

$$C_a = f \cdot C_w \tag{1}$$

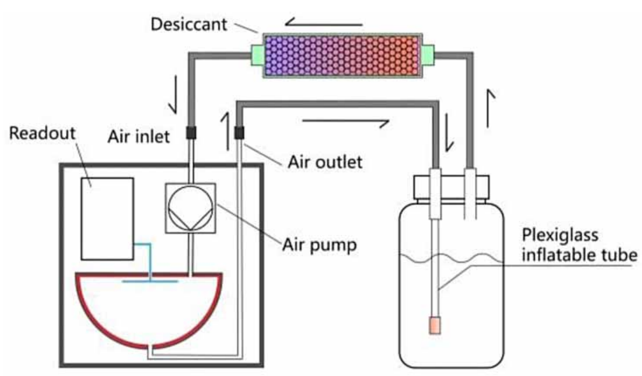

Figure 1 | Structure and principle of FD216 environmental radon concentration measuring instrument.

where C_a is the concentration of radon in indoor air produced by water (Bq m^{-3}), f is the transfer factor, C_w is the concentration of radon in tap water (Bq m^{-3}) (Nazaroff *et al.* 1987):

$$f = (W \cdot e)/(\lambda \cdot V) \tag{2}$$

where W is the per capita water consumption of residents (m^3 h^{-1}), e is the release rate of radon from tap water into the air, with a value of 0.55, the ventilation rate of the dwelling λ is 0.68 h^{-1}, and V is the volume of the dwelling (m^3) (Nazaroff *et al.* 1987).

The concentration of partial short-lived progenies of ^{222}Rn diffused into the air using Equations (3) and (4):

$$c_{j+1} = d_j \cdot c_j \tag{3}$$

$$d_j = \lambda_{j+1}/[\lambda_{j+1} + L + h_{j+1} \cdot q_a + (1 - h_{j+1}) \cdot q_u] \tag{4}$$

where $j = 0, 1, 2, 3, 4$, $c_{j=0}$ is the concentration of ^{222}Rn in air (Bq m^{-3}), and c_j is the concentration of ^{222}Rn's jth progeny in air (Bq m^{-3}), λ_{j+1} is the disintegration constant of the $j+1$th progeny, L is the ventilation rate of the dwelling (h^{-1}), h_{j+1} is the ratio of the concentration of the attached $j+1$th progeny on aerosols to the total concentration of the attached and unattached radon progenies, $h_1 = 0.9$ and $h_2 = h_3 = h_4 = 1$, q_a and q_u are the deposition rates of the attached and unattached progenies, $q_a = 7.5 \times 10^{-5}(s^{-1})$, and $q_u = 8.33 \times 10^{-3}$ (s^{-1}) (Planinić *et al.* 1997; Misdaq *et al.* 2012).

2.3. Estimation of the committed effective dose of radon and its progenies

Figure 2 shows the human respiratory tract model and part of human digestive tract model provided by ICRP publication (ICRP 2015).

Compartment ET_1: retention of material deposited in the anterior nose (region ET_1); compartment ET_{seq}: long-term retention in airway tissue of a small fraction of particles deposited in the nasal passages (region ET_2); compartment ET'_2: short-term retention of the material deposited in the posterior nasal passage, larynx, and pharynx (ET_2 region); compartment BB': retention of particles in the bronchial (region BB), with particle transport to ET'_2; compartment bb': retention of particles in the bronchiole (region bb), with particle transport to BB'; compartment BBseq: long-term retention in airway walls of a small fraction of the particles deposited in the bronchiole (region bb); compartment bbseq: long-term retention in airway walls of a small fraction of the particles deposited in the bronchiole (region bb); compartment ALV: retention of particles deposited in the alveoli. INT: long-term retention of the particles deposited in the alveoli that penetrate to the interstitium: the particles are removed slowly to the lymph nodes (ICRP 2015).

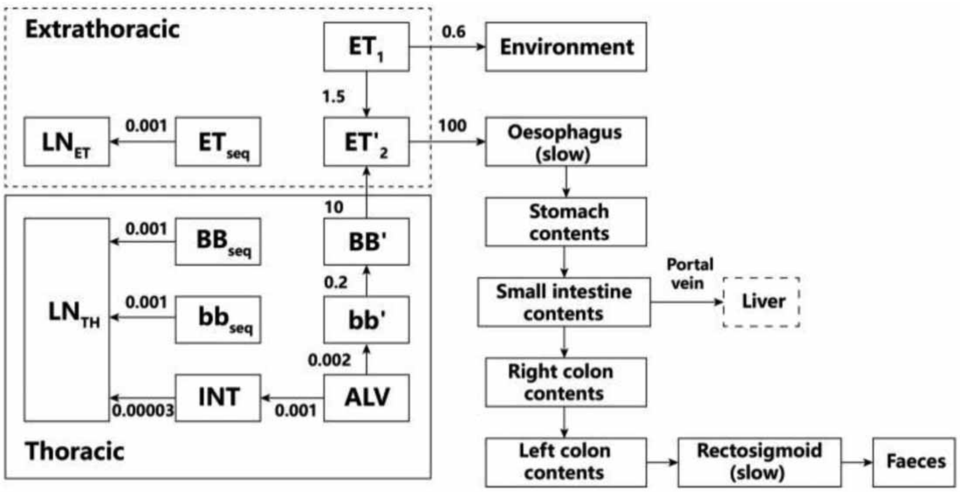

Figure 2 | Compartment model representing time-dependent particle transport from each region. The transport rates shown alongside arrows are reference values in units of d^{-1}, the combined model of the human respiratory tract and alimentary tract refers to ICRP Publication 130 (ICRP 2015).

The rate of change of the *j*th decay progeny of ^{222}Rn in the *i*th compartment of the respiratory tract is given by the following equation:

$$dA_c^i(j)/dt = F_d(i) \cdot I(j) + \sum_n \lambda_{n,i} \cdot A_c^n(j) - \left(\sum_n \lambda_{i,n} + \lambda_j \right) \cdot A_c^i(j) \quad (5)$$

where $A_c^i(j)$ is the radioactive activity of the *j*th decay progeny of ^{222}Rn in the *i*th compartment of the respiratory tract, $F_d(i)$ is the fractional deposition in the compartment *i* of the respiratory tract of different members of the public, $I(j) = B \cdot A_C(j)$. *B* is the average breathing rate for different members of the public ($m^3\ h^{-1}$). $A_C(j)$ is the radioactive activity of the *j*th decay progeny ($Bq\ m^{-3}$), $\lambda_{n,i} = m_{n,i}$, where $m_{n,i}$ is the clearance rate from regions *n* to *i* due to particle transport. $\lambda_{i,n} = m_{i,n} + f_r \cdot S_r + (1 - f_r) \cdot S_s$, where $m_{i,n}$ is the clearance rate from regions *i* to *n* due to particle transport, f_r is the fraction dissolved into the blood relatively rapidly, at a rate S_r (d^{-1}), $(1 - f_r)$ is the fraction dissolved into the blood relatively slowly, at a rate S_s (d^{-1}). Except for the anterior nasal passage (ET_1), the deposit from other regions of the respiratory tract is absorbed into the blood at a certain rate, and the dissolution rates of different radon progenies are different, in the process of ^{214}Pb dissolving into the blood, a certain proportion of particles will first transform into 'bound' state. λ_j is the radioactive constant of the *j*th decay progeny of ^{222}Rn (ICRP 2002a, 2015; Misdaq & Flata 2003).

The rate of change of the *j*th decay progeny of ^{222}Rn in the *i*th compartment of the alimentary tract is given by the following equation:

$$dA_c^i(j)/dt = \sum_n m_{n,i} \cdot A_c^n(j) - \left(\sum_n \lambda_{i,n} + \lambda \right) \cdot A_c^i(j) \quad (6)$$

where $\lambda_{i,n} = m_{i,n} + \lambda_{i,b}$, $m_{i,n}$ is the transport rate from regions *i* to *n*, and $\lambda_{i,b}$ is the rate of blood absorption in organ or tissue *i*, for material cleared from the respiratory tract to the alimentary tract, the fractional absorption in the alimentary tract is the product of f_r and f_A, where f_A is the fractional absorption in the alimentary tract for relatively soluble forms of the element (ICRP 2015).

Then the committed equivalent doses of the *j*th decay progeny of ^{222}Rn in the target region *T* are given by the following equations:

$$H_T(j)(\tau) = \int_0^\tau \dot{H}_T(j)(t)d(t) \quad (7)$$

$$\dot{H}_T(j)(t) = k \cdot A_C^T(j)(t) \cdot w_R \cdot Y_j \cdot E_j \cdot SAF \quad (8)$$

where $\dot{H}_T(j)(t)$ is the equivalent dose rate of the *j*th decay progeny of ^{222}Rn, $A_C^T(j)(t)$ is the radioactive activity of the *j*th decay progeny of ^{222}Rn in the target region *T* of the respiratory tract (Bq), w_R is the radiation-weighting factor, α-particle is 20, β-particle is 1. $k = 1.6 \times 10^{-13}$ ($J\ MeV^{-1}$) is the joule to electron volt conversion factor, Y_j is the yield of the *j*th decay progeny of ^{222}Rn ($(Bq\ s)^{-1}$), E_j is the energy of the *j*th decay progeny of ^{222}Rn (MeV), *SAF* is the specific absorbed fraction (kg^{-1}), τ is the exposure time of the target region *T* (ICRP 2016).

Equations (9) and (10) are used to calculate the committed equivalent dose of the extrathoracic region and the thoracic region, respectively. Equation (11) is used to calculate the committed equivalent dose of the colon region:

$$H_{ET}(j)(\tau) = H_{ET_1}(j)(\tau) \cdot A_{ET_1} + H_{ET_2}(j)(\tau) \cdot A_{ET_2} + H_{LN_{ET}}(j)(\tau) \cdot A_{LN_{ET}} \quad (9)$$

$$H_{TH}(j)(\tau) = H_{BB}(j)(\tau) \cdot A_{BB} + H_{bb}(j)(\tau) \cdot A_{bb} + H_{AI}(j)(\tau) \cdot A_{AI} + H_{LN_{TH}}(j)(\tau) \cdot A_{LN_{TH}} \quad (10)$$

$$H_{colon}(j)(\tau) = H_{RC}(j)(\tau) \cdot A_{RC} + H_{LC}(j)(\tau) \cdot A_{LC} + H_{RS}(j)(\tau) \cdot A_{RS} \quad (11)$$

where $H_{ET_1}(j)(\tau)$ is the committed equivalent dose of the *j*th decay progeny of ^{222}Rn in the ET_1 region, A_{ET_1} represents the ET_1 region's estimated radiosensitivity relative to that of the whole organ, $A_{ET_1} = A_{LN_{ET}} = 0.001$, $A_{ET_2} = 0.998$, $A_{BB} = A_{bb} = A_{AI} = 0.333$, $A_{LN_{TH}} = 0.001$, $A_{RC} = A_{LC} = 0.4$, and $A_{RS} = 0.2$ (ICRP 1994, 2002a).

The committed effective dose of the jth decay progeny of ^{222}Rn is given by the following equation:

$$E(j)(\tau) = \sum_{T} w_T \cdot H_T(j)(\tau) \tag{12}$$

where the tissue-weighting factor w_T for $H_{ET}(j)(\tau)$ is 0.025, the tissue-weighting factor w_T for $H_{TH}(j)(\tau)$ is 0.12, for organs of the alimentary tract other than the esophagus, the tissue-weighting factor w_T is 0.12, while the tissue-weighting factor of the esophagus is 0.04 (ICRP 2002a).

According to the gastrointestinal system provided by ICRP Publication (ICRP 1979), as shown in Figure 3, the whole gastrointestinal system comprises five regions: stomach, small intestine, upper large intestine, lower large intestine, and blood.

The rate of change of ^{222}Rn in the ith compartment of the alimentary tract is given by the following equation:

$$dA_c^i(^{222}\text{Rn})/dt = \sum_{n} m_{n,i} \cdot A_c^n(^{222}\text{Rn}) - \left(\sum_{n} \lambda_{i,n} + \lambda\right) \cdot A_c^i(^{222}\text{Rn}) \tag{13}$$

where $A_c^i(^{222}\text{Rn})$ is the activity of ^{222}Rn in the ith compartment of the alimentary tract, $m_{n,i}$ is the transport rate from regions n to i, $\lambda_{i,n} = m_{i,n} + \lambda_{i,b}$, $m_{i,n}$ is the transport rate from regions i to n and $\lambda_{i,b}$ is the rate of blood absorption in the organ or tissue i, and λ is the radioactive constant of the ^{222}Rn (ICRP 2015).

The committed equivalent doses of ^{222}Rn in the tissue T of the alimentary tract are given by the following equations:

$$H_T(^{222}\text{Rn})(\tau) = \int_0^{\tau} \dot{H}_T(^{222}\text{Rn})(t)d(t) \tag{14}$$

$$\dot{H}_T(^{222}\text{Rn})(t) = 0.01 \cdot A_C^T(^{222}\text{Rn})(t) \cdot w_R \cdot k \cdot K_j \cdot S_j \cdot R_j/m_T \tag{15}$$

where $\dot{H}_T(^{222}\text{Rn})(t)$ is the equivalent dose rate of ^{222}Rn, 0.01 is assuming that only 1% of the contents of α-particle will cause a dose to any of the walls of the gastrointestinal tract, $A_C^T(^{222}\text{Rn})(t)$ is the radioactive activity of ^{222}Rn in the tissue T of the respiratory tract (Bq), w_R is the radiation-weighting factor, $k = 1.6 \times 10^{-13}$ (J MeV^{-1}) is the electron volt to joule conversion factor, K_j is the branching ratio for ^{222}Rn disintegration, S_j is the stopping power of the tissue T for the α-particles emitted by ^{222}Rn (MeV cm^2 g^{-1}), R_j is the range of the α-particles emitted by ^{222}Rn in the tissue of the target organ (g cm^{-2}), m_T is the mass of tissue T (kg), and τ is the exposure time of the tissue T (ICRP 2002b).

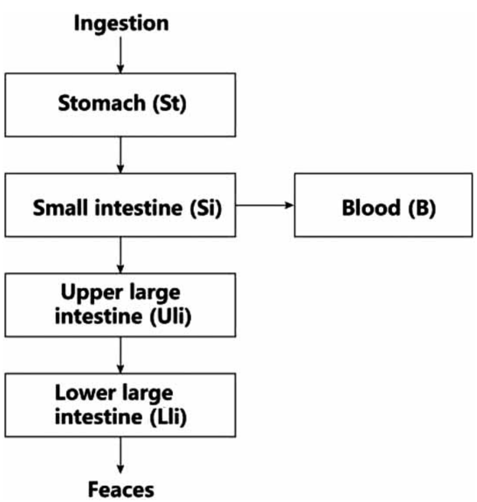

Figure 3 | Structure of the gastrointestinal system. The model refers to ICRP Publication 30 (ICRP 1979).

The committed effective dose of the *j*th decay progeny of ^{222}Rn is given by the following equation:

$$E(^{222}Rn)(\tau) = \sum_{T} w_T \cdot H_T(^{222}Rn)(\tau) \quad (16)$$

3. RESULT AND DISCUSSION

3.1. Radon concentration in residential tap water

The radon concentrations of tap water in residential buildings at different temperatures are shown in Table 1. The radon concentration of residential tap water ranges from 280 to 750 mBq L^{-1}, with an average value of 548.16 mBq L^{-1}, among them, the radon concentration of tap water sample L5 is the highest, and that of L6 is the lowest, which is 738 ± 20.2 and 288 ± 7.6 mBq L^{-1}, respectively. Radon concentrations in all tap water samples were consistent with the USEPA's maximum contaminant level of 11.11 Bq L^{-1} and the drinking water radon parameter (100 Bq L^{-1}) set by the EURATOM Drinking-Water Directive (USEPA 1999; Council Directive 2013/51/Euratom 2013). Radon concentrations in tap water in some countries and regions are shown in Table 2, and it is obvious that the measurement results of this study are within the range of those measured in these countries and regions (Sarrou & Pashalidis 2003; Marques *et al.* 2004; Rusconi *et al.* 2004; Pagava *et al.* 2008; Nita *et al.* 2013; Ahmad *et al.* 2015; Erdogan *et al.* 2015; Fakhri *et al.* 2015; Le *et al.* 2015).

3.2. Variation of radon concentration in tap water at different temperatures

In this study, tap water samples from different residential buildings will be gradually heated to 25, 40, 55, 70, 85, and 100 °C by water bath heating. Radon concentrations at different temperatures are shown in Table 3. The radon concentration in the

Table 1 | Radon concentrations (mBq L^{-1}) of tap water in residential buildings

Sample code	Temperature (°C)	Radon concentration (mBq L^{-1})
L1	24.5	376 ± 23.6
L2	24.3	456 ± 15.0
L3	24.8	720 ± 85.4
L4	24.0	710 ± 17.3
L5	24.4	738 ± 20.2
L6	24.1	288 ± 7.6
Average		548.16

Table 2 | Radon concentrations (mBq L^{-1}) in tap water in different countries or regions

Location	Radon concentration (mBq L^{-1})	References
Konya, Turkey	870–18,340	Erdogan *et al.* (2015)
Minab, Iran	200–1,710	Fakhri *et al.* (2015)
Ho Chi Minh, Vietnam	30–205	Le *et al.* (2015)
Sungai Petani, Kedah, Malaysia	2,390–8,010	Ahmad *et al.* (2015)
Cyprus	100–2,000	Sarrou & Pashalidis (2003)
Brazil	340–510	Marques *et al.* (2004)
Transylvania, Romania	1,200–4,500	Nita *et al.* (2013)
Milano, Italy	390–690	Rusconi *et al.* (2004)
Tbilisi, Georgia	3,000–5,000	Pagava *et al.* (2008)
Urumqi, China	280–750	Present study

Table 3 | Radon concentrations (mBq L^{-1}) of tap water in residential buildings at different temperatures

	Radon concentration (mBq L^{-1})					
Sample code	**25 °C**	**40 °C**	**55 °C**	**70 °C**	**85 °C**	**100 °C**
L1	370 ± 26.5	240 ± 10.0	187 ± 11.5	110 ± 10.0	120 ± 26.4	123 ± 5.8
L2	453 ± 15.3	306 ± 25.1	267 ± 20.8	143 ± 5.8	163 ± 20.8	133 ± 58.5
L3	723 ± 75.1	263 ± 20.8	297 ± 73.7	180 ± 17.3	210 ± 26.5	177 ± 25.2
L4	700 ± 75.5	287 ± 30.6	213 ± 32.1	217 ± 64.3	237 ± 32.1	137 ± 37.9
L5	730 ± 43.6	237 ± 30.6	260 ± 55.7	213 ± 20.8	213 ± 15.2	93 ± 25.4
L6	283 ± 11.5	190 ± 10.0	137 ± 25.2	63 ± 20.8	77 ± 25.1	33 ± 15.2
Average	543.33	253.89	226.67	154.44	170.00	116.11

six groups of tap water samples showed an obvious downward trend on the whole with the increase of the water bath temperature. The average radon concentration at 25 °C was 543.33 mBq L^{-1}, and it decreased to 116.11 mBq L^{-1} at 100 °C. The variation of the radon retention rate (radon concentration at a certain water bath temperature/initial radon concentration × 100%) in tap water at different water bath temperatures is shown in Figure 4, radon retention decreases with the gradual increase of temperature too, when the temperature reaches 100 °C, the average radon retention rate in the sample group is only 21.99%. The results indicate that heating tap water can effectively reduce the concentration of radon in water and reduce the harm of radon intake to public health.

Despite there were two different trends, the concentration of radon in the samples decreased after water bath heating. Due to the low initial radon concentration (the average value is 368.89 mBq L^{-1}), the radon retention rates of samples L1, L2, and L6 decrease continuously from 40 to 70 °C and then change gently. However, the radon retention rate of samples L3, L4, and L5 (with an average radon concentration of 717.78 mBq L^{-1}) with a high initial radon concentration decreased rapidly between 25 and 40 °C, and then the change was flat. The radon concentration and retention rate of the six sample groups

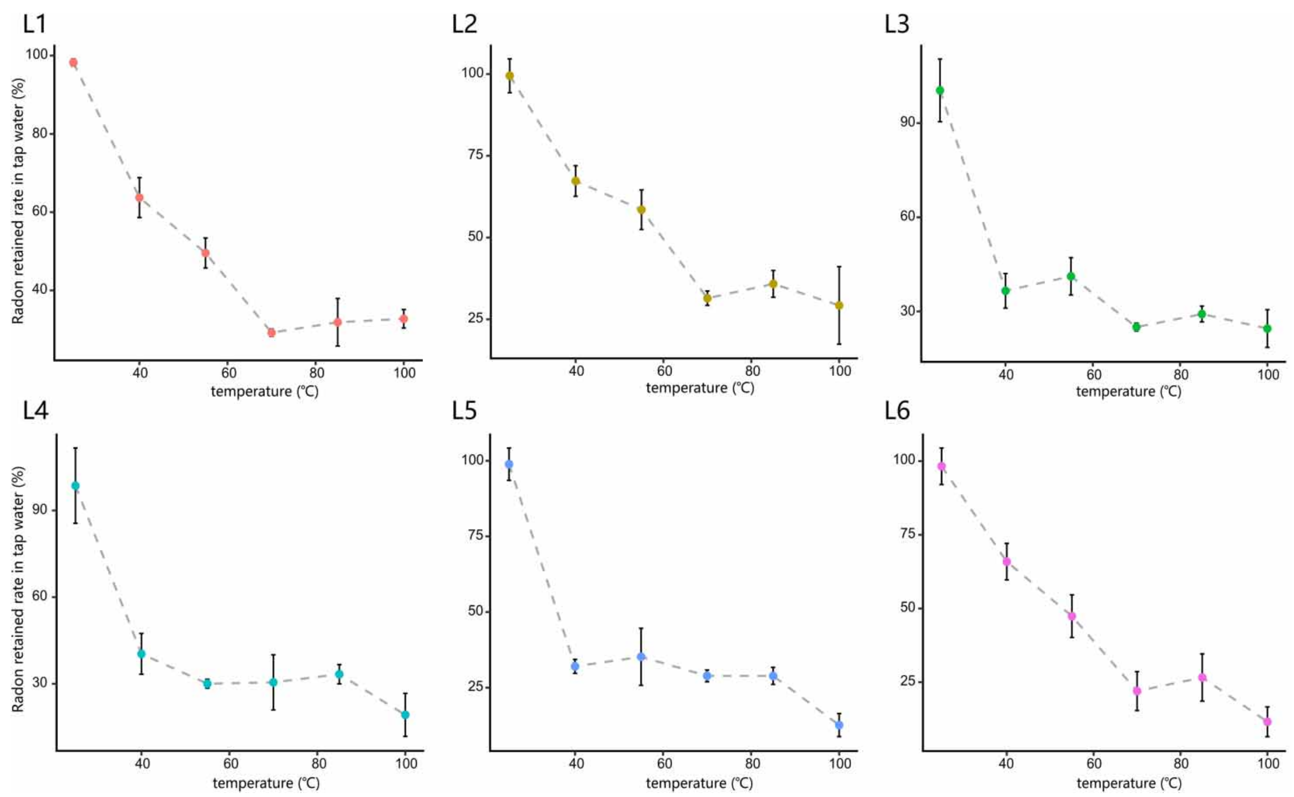

Figure 4 | Variation of radon retention rate of tap water samples at different temperatures.

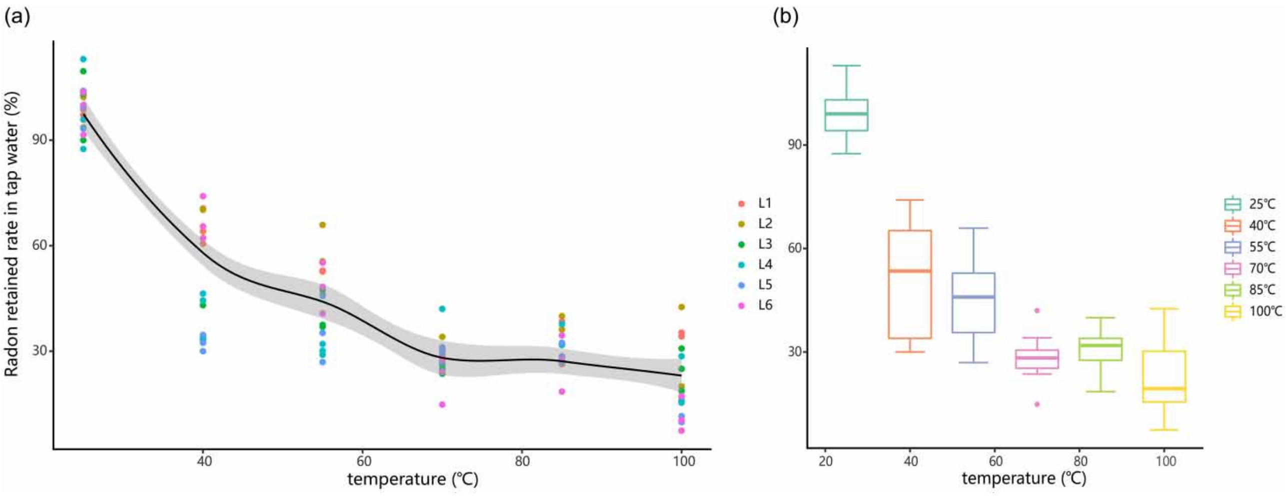

Figure 5 | (a) Fitting curve of the change of radon retention rate of tap water samples at different temperatures. (b) Boxplot of radon retention rates at different temperatures.

increased slightly from 70 to 85 °C. Statistical analysis showed that there was no significant difference in the radon concentration value and the radon retention rate between 70 and 85 °C ($p < 0.05$).

The radon retention rates of all samples at different temperatures were fitted by the method of locally weighted regression (LOESS), as shown in Figure 5. When the water bath heating temperature changes from 25 to 70 °C, with the increase in temperature, radon retention decreases continuously, dropping to only about 30%. With the increase of water bath

Table 4 | Annual committed equivalent dose due to inhalation of radon decay progenies ^{218}Po, ^{214}Pb, ^{214}Bi, and ^{214}Po during the bath to adult male respiratory target tissues

		Annual committed equivalent dose (μSv a^{-1})						
Sample code	**Decay progenies of ^{222}Rn**	**ET_1**	**ET_2**	**LN_{ET}**	**BB**	**bb**	**AI**	**LN_{TH}**
L1	^{218}Po	125.65	1.21	1.84×10^{-8}	0.26	2.19	9.86×10^{-2}	0.83×10^{-8}
	^{214}Pb	0.98	5.48×10^{-2}	2.53×10^{-4}	3.59×10^{-3}	1.94×10^{-3}	5.88×10^{-4}	2.63×10^{-5}
	^{214}Bi	0.48	2.34×10^{-2}	6.88×10^{-4}	2.14×10^{-3}	1.34×10^{-3}	7.77×10^{-4}	1.08×10^{-4}
	^{214}Po	2.68×10^{-4}	2.51×10^{-6}	1.13×10^{-20}	7.19×10^{-7}	1.02×10^{-6}	5.61×10^{-8}	5.14×10^{-21}
L2	^{218}Po	160.56	1.55	2.35×10^{-8}	0.34	2.80	1.26×10^{-1}	1.06×10^{-8}
	^{214}Pb	1.25	7.01×10^{-2}	3.23×10^{-4}	4.59×10^{-3}	2.48×10^{-3}	7.51×10^{-4}	3.36×10^{-5}
	^{214}Bi	0.61	2.99×10^{-2}	8.79×10^{-4}	2.73×10^{-3}	1.72×10^{-3}	9.93×10^{-4}	1.38×10^{-4}
	^{214}Po	3.42×10^{-4}	3.21×10^{-6}	1.45×10^{-20}	9.19×10^{-7}	1.31×10^{-6}	7.17×10^{-8}	6.57×10^{-21}
L3	^{218}Po	137.87	1.33	2.02×10^{-8}	0.29	2.41	1.08×10^{-1}	0.91×10^{-8}
	^{214}Pb	1.08	6.02×10^{-2}	2.78×10^{-4}	3.94×10^{-3}	2.13×10^{-3}	6.45×10^{-4}	2.89×10^{-5}
	^{214}Bi	0.52	2.57×10^{-2}	7.54×10^{-4}	2.35×10^{-3}	1.47×10^{-3}	8.52×10^{-4}	1.18×10^{-4}
	^{214}Po	2.94×10^{-4}	2.76×10^{-6}	1.24×10^{-20}	7.89×10^{-7}	1.12×10^{-6}	6.16×10^{-8}	5.64×10^{-21}
L4	^{218}Po	150.09	1.45	2.20×10^{-8}	0.32	2.62	1.17×10^{-1}	0.99×10^{-8}
	^{214}Pb	1.17	6.55×10^{-2}	3.02×10^{-4}	4.29×10^{-3}	2.32×10^{-3}	7.02×10^{-4}	3.14×10^{-5}
	^{214}Bi	0.57	2.80×10^{-2}	8.21×10^{-4}	2.55×10^{-3}	1.61×10^{-3}	9.28×10^{-4}	1.29×10^{-4}
	^{214}Po	3.20×10^{-4}	3.00×10^{-6}	1.35×10^{-20}	8.59×10^{-7}	1.22×10^{-6}	6.71×10^{-8}	6.14×10^{-21}
L5	^{218}Po	123.91	1.19	1.81×10^{-8}	0.26	2.16	0.97×10^{-1}	0.82×10^{-8}
	^{214}Pb	0.97	5.41×10^{-2}	2.49×10^{-4}	3.54×10^{-3}	1.91×10^{-3}	5.80×10^{-4}	2.60×10^{-5}
	^{214}Bi	0.47	2.31×10^{-2}	6.78×10^{-4}	2.11×10^{-3}	1.32×10^{-3}	7.66×10^{-4}	1.06×10^{-4}
	^{214}Po	2.64×10^{-4}	2.48×10^{-6}	1.12×10^{-20}	7.09×10^{-7}	1.01×10^{-6}	5.53×10^{-8}	5.07×10^{-21}
L6	^{218}Po	99.47	0.96	1.46×10^{-8}	0.21	1.73	0.78×10^{-1}	0.66×10^{-8}
	^{214}Pb	0.78	4.34×10^{-2}	2.01×10^{-4}	2.84×10^{-3}	1.53×10^{-3}	4.65×10^{-4}	2.08×10^{-5}
	^{214}Bi	0.38	1.85×10^{-2}	5.44×10^{-4}	1.69×10^{-3}	1.06×10^{-3}	6.15×10^{-4}	0.85×10^{-4}
	^{214}Po	2.12×10^{-4}	1.99×10^{-6}	0.89×10^{-20}	5.69×10^{-7}	0.81×10^{-6}	4.44×10^{-8}	4.07×10^{-21}

temperature, the declining trend of radon retention is gentle, and the fitting curve is flat between 70 and 85 °C, followed by a slow decline between 85 and 100 °C, which possibly was because blisters appeared in the heated samples as the water bath temperature increased, accelerating radon degassing in the water.

3.3. Estimation of the committed equivalent and effective dose of residential tap water

The annual committed equivalent dose and effective dose of radon and its progenies in tap water to respiratory and alimentary tract organs or tissues were estimated.

According to the actual situation of resident residence, bathroom space is about 14 m^3. Meanwhile, according to the actual water consumption habits of residents, the temperature of shower water is assumed to be 40 °C, 30 min of shower three times a week, the water consumption is about 0.36 $m^3 \cdot h^{-1}$, and the decay progenies of radon released into the air during the shower are attached to the particles with an activity median aerodynamic diameter (AMAD) of 1 μm. The annual drinking water quantity of adult residents is 500 L, and the tap water will be boiled and cooled for drinking, ignoring the part of the indoor air radon dissolves into the tap water during cooling, the study assumes that all the radon concentrations taken in are the values at 100 °C and appear in the stomach (UNSCEAR 2000; ICRP 2002a).

The committed equivalent dose of inhalation of α decay short-lived progenies (^{218}Po and ^{214}Po) and β decay short-lived progenies (^{214}Pb and ^{214}Bi) to the respiratory tract and alimentary tract target tissues during a shower is shown in Tables 4–6. The committed equivalent dose contribution of α-particles to ET_1, ET_2, BB, bb, and AI in the respiratory tissue regions was higher than that of β-particles. The committed equivalent doses of β-particles to the target tissues of the respiratory tract are close to each other in order of magnitude, and the committed equivalent dose to LN_{ET} and LN_{TH} regions is higher than that of the α-particles. In the alimentary tract, the committed equivalent dose of ^{214}Pb to the target tissues of the esophagus was higher than that of ^{214}Bi, while that to other organs of the alimentary tract was lower than ^{214}Bi.

Due to different respiratory rates (0.54 $m^3 \cdot h^{-1}$ for adult males and 0.39 $m^3 \cdot h^{-1}$ for adult females) and SAF, the committed equivalent dose contribution of short-lived progenies to all tissue regions of the adult male respiratory tract (except region

Table 5 | Annual committed equivalent dose due to inhalation of radon decay progenies ^{218}Po, ^{214}Pb, ^{214}Bi, and ^{214}Po during the bath to adult female respiratory tract target tissues

		Annual committed equivalent dose (μSv a^{-1})						
Sample code	**Decay progenies of ^{222}Rn**	**ET_1**	**ET_2**	**LN_{ET}**	**BB**	**bb**	**AI**	**LN_{TH}**
L1	^{218}Po	80.83	0.71	1.86×10^{-8}	0.17	1.96	7.49×10^{-2}	0.85×10^{-8}
	^{214}Pb	0.82	4.64×10^{-2}	4.55×10^{-5}	2.89×10^{-3}	1.61×10^{-3}	4.75×10^{-4}	1.16×10^{-4}
	^{214}Bi	0.40	1.96×10^{-2}	1.36×10^{-4}	1.71×10^{-3}	1.02×10^{-3}	6.30×10^{-4}	4.41×10^{-4}
	^{214}Po	2.24×10^{-4}	2.34×10^{-6}	1.14×10^{-20}	5.54×10^{-7}	9.07×10^{-7}	4.27×10^{-8}	5.25×10^{-21}
L2	^{218}Po	103.14	0.90	2.38×10^{-8}	0.22	2.51	9.58×10^{-2}	1.09×10^{-8}
	^{214}Pb	1.05	5.93×10^{-2}	5.82×10^{-5}	3.70×10^{-3}	2.06×10^{-3}	6.07×10^{-4}	1.48×10^{-4}
	^{214}Bi	0.52	2.51×10^{-2}	1.74×10^{-4}	2.19×10^{-3}	1.317×10^{-3}	8.05×10^{-4}	5.63×10^{-4}
	^{214}Po	2.86×10^{-4}	2.98×10^{-6}	1.46×10^{-20}	7.08×10^{-7}	1.15×10^{-6}	5.45×10^{-8}	6.72×10^{-21}
L3	^{218}Po	88.57	0.77	2.04×10^{-8}	0.18	2.15	8.22×10^{-2}	0.93×10^{-8}
	^{214}Pb	0.90	5.09×10^{-2}	4.99×10^{-5}	3.17×10^{-3}	1.76×10^{-3}	5.21×10^{-4}	1.27×10^{-4}
	^{214}Bi	0.45	2.16×10^{-2}	1.49×10^{-4}	1.88×10^{-3}	1.12×10^{-3}	6.91×10^{-4}	4.83×10^{-4}
	^{214}Po	2.45×10^{-4}	2.56×10^{-6}	1.25×10^{-20}	6.07×10^{-7}	9.95×10^{-7}	4.68×10^{-8}	5.77×10^{-21}
L4	^{218}Po	96.42	0.84	2.22×10^{-8}	0.20	2.34	8.95×10^{-2}	1.02×10^{-8}
	^{214}Pb	0.98	5.54×10^{-2}	5.45×10^{-5}	3.46×10^{-3}	1.92×10^{-3}	5.67×10^{-4}	1.38×10^{-4}
	^{214}Bi	0.41	2.35×10^{-2}	1.63×10^{-4}	2.04×10^{-3}	1.22×10^{-3}	7.53×10^{-4}	5.26×10^{-4}
	^{214}Po	2.67×10^{-4}	2.79×10^{-6}	1.36×10^{-20}	6.61×10^{-7}	1.08×10^{-6}	5.10×10^{-8}	6.28×10^{-21}
L5	^{218}Po	79.60	0.69	1.83×10^{-8}	0.16	1.93	7.39×10^{-2}	0.84×10^{-8}
	^{214}Pb	0.81	4.57×10^{-2}	4.50×10^{-5}	2.85×10^{-3}	1.59×10^{-3}	4.68×10^{-4}	1.14×10^{-4}
	^{214}Bi	0.39	1.94×10^{-2}	1.34×10^{-4}	1.69×10^{-3}	1.01×10^{-3}	6.21×10^{-4}	4.34×10^{-4}
	^{214}Po	2.21×10^{-4}	2.31×10^{-6}	1.13×10^{-20}	5.46×10^{-7}	8.94×10^{-7}	4.21×10^{-8}	5.18×10^{-21}
L6	^{218}Po	63.91	0.55	1.47×10^{-8}	0.13	1.55	5.93×10^{-2}	0.67×10^{-8}
	^{214}Pb	0.65	3.67×10^{-2}	3.61×10^{-5}	2.29×10^{-3}	1.27×10^{-3}	3.76×10^{-4}	0.92×10^{-4}
	^{214}Bi	0.31	1.55×10^{-2}	1.08×10^{-4}	1.35×10^{-3}	0.81×10^{-3}	4.99×10^{-4}	3.49×10^{-4}
	^{214}Po	1.77×10^{-4}	1.85×10^{-6}	0.91×10^{-20}	4.38×10^{-7}	7.18×10^{-7}	3.38×10^{-8}	4.16×10^{-21}

Table 6 | Annual committed equivalent dose due to inhalation of radon decay progenies during the bath to alimentary tract target tissues

Sample code	Gender	Decay progenies of ^{222}Rn	Annual committed equivalent dose ($\mu Sv\ a^{-1}$)					
			Oesophagus	Stomach	Small intestine	Right colon	Left colon	Rectosigmoid
L1	Adult male	^{214}Pb	4.27×10^{-3}	1.13×10^{-3}	4.23×10^{-5}	1.78×10^{-6}	2.54×10^{-7}	3.45×10^{-8}
		^{214}Bi	3.20×10^{-3}	1.75×10^{-3}	5.97×10^{-5}	4.28×10^{-6}	6.27×10^{-7}	8.73×10^{-8}
	Adult female	^{214}Pb	3.38×10^{-3}	0.87×10^{-3}	3.62×10^{-5}	1.53×10^{-6}	1.37×10^{-7}	2.08×10^{-7}
		^{214}Bi	2.56×10^{-3}	1.33×10^{-3}	4.94×10^{-5}	3.45×10^{-6}	2.98×10^{-7}	5.60×10^{-7}
L2	Adult male	^{214}Pb	5.46×10^{-3}	1.45×10^{-3}	5.55×10^{-5}	2.35×10^{-6}	3.32×10^{-7}	4.55×10^{-8}
		^{214}Bi	4.09×10^{-3}	2.24×10^{-3}	7.63×10^{-5}	5.48×10^{-6}	8.02×10^{-7}	1.11×10^{-7}
	Adult female	^{214}Pb	4.31×10^{-3}	1.11×10^{-3}	4.63×10^{-5}	1.96×10^{-6}	1.75×10^{-7}	2.63×10^{-7}
		^{214}Bi	3.27×10^{-3}	1.70×10^{-3}	6.32×10^{-5}	4.43×10^{-6}	3.82×10^{-7}	7.12×10^{-7}
L3	Adult male	^{214}Pb	4.69×10^{-3}	1.24×10^{-3}	4.77×10^{-5}	2.02×10^{-6}	2.85×10^{-7}	3.91×10^{-8}
		^{214}Bi	3.51×10^{-3}	1.92×10^{-3}	6.55×10^{-5}	4.69×10^{-6}	6.88×10^{-7}	9.59×10^{-8}
	Adult female	^{214}Pb	3.71×10^{-3}	0.95×10^{-3}	3.98×10^{-5}	1.68×10^{-6}	1.50×10^{-7}	2.26×10^{-7}
		^{214}Bi	2.81×10^{-3}	1.46×10^{-3}	5.33×10^{-5}	3.81×10^{-6}	3.29×10^{-7}	6.12×10^{-7}
L4	Adult male	^{214}Pb	5.10×10^{-3}	1.35×10^{-3}	5.19×10^{-5}	2.20×10^{-6}	3.11×10^{-7}	4.25×10^{-8}
		^{214}Bi	3.82×10^{-3}	2.09×10^{-3}	7.02×10^{-5}	5.13×10^{-6}	7.49×10^{-7}	1.04×10^{-7}
	Adult female	^{214}Pb	4.03×10^{-3}	1.04×10^{-3}	4.33×10^{-5}	1.83×10^{-6}	1.63×10^{-7}	2.46×10^{-7}
		^{214}Bi	3.05×10^{-3}	1.59×10^{-3}	5.90×10^{-5}	4.13×10^{-6}	3.50×10^{-7}	6.69×10^{-7}
L5	Adult male	^{214}Pb	4.21×10^{-3}	1.12×10^{-3}	4.29×10^{-5}	1.76×10^{-6}	2.51×10^{-7}	3.41×10^{-8}
		^{214}Bi	3.15×10^{-3}	1.72×10^{-3}	5.88×10^{-5}	4.22×10^{-6}	6.18×10^{-7}	8.61×10^{-8}
	Adult female	^{214}Pb	3.33×10^{-3}	0.85×10^{-3}	3.57×10^{-5}	1.51×10^{-6}	1.35×10^{-7}	2.03×10^{-7}
		^{214}Bi	2.52×10^{-3}	1.31×10^{-3}	4.87×10^{-5}	3.41×10^{-6}	2.94×10^{-7}	5.53×10^{-7}
L6	Adult male	^{214}Pb	3.38×10^{-3}	0.89×10^{-3}	3.43×10^{-5}	1.45×10^{-6}	2.05×10^{-7}	2.81×10^{-8}
		^{214}Bi	2.53×10^{-3}	1.38×10^{-3}	4.72×10^{-5}	3.39×10^{-6}	4.96×10^{-7}	6.92×10^{-8}
	Adult female	^{214}Pb	2.67×10^{-3}	0.68×10^{-3}	2.86×10^{-5}	1.21×10^{-6}	1.08×10^{-7}	1.63×10^{-7}
		^{214}Bi	2.02×10^{-3}	1.05×10^{-3}	3.91×10^{-5}	2.73×10^{-6}	2.36×10^{-7}	4.44×10^{-7}

LN_{TH}) was higher than that of the adult female. In the alimentary tract, except for the rectosigmoid, the committed equivalent dose in the target region of other organs was higher in adult males than in adult females.

The average annual cumulative effective dose of the respiratory tract and digestive tract in males was 0.125 and 6.97×10^{-4} $\mu Sv\ a^{-1}$, respectively, and that of females was 0.104 and 5.43×10^{-4} $\mu Sv\ a^{-1}$. The average total annual committed effective dose was 0.126 $\mu Sv\ a^{-1}$ for adult male and 0.105 $\mu Sv\ a^{-1}$ for an adult female (as shown in Table 7), the annual committed

Table 7 | Annual committed effective dose due to inhalation of radon decay progenies (^{218}Po, ^{214}Pb, ^{214}Bi, and ^{214}Po) during the bath

Sample code	Gender	Annual committed effective dose ($\mu Sv\ a^{-1}$)		
		Respiratory tract	Alimentary tract	Total
L1	Adult male	1.18×10^{-1}	6.58×10^{-4}	1.19×10^{-1}
	Adult female	0.99×10^{-1}	5.13×10^{-4}	0.99×10^{-1}
L2	Adult male	1.51×10^{-1}	8.41×10^{-4}	1.52×10^{-1}
	Adult female	1.26×10^{-1}	6.55×10^{-4}	1.27×10^{-1}
L3	Adult male	1.30×10^{-1}	7.22×10^{-4}	$1.30a \times 10^{-1}$
	Adult female	1.08×10^{-1}	5.62×10^{-4}	1.09×10^{-1}
L4	Adult male	1.41×10^{-1}	7.86×10^{-4}	1.42×10^{-1}
	Adult female	1.18×10^{-1}	6.12×10^{-4}	1.18×10^{-1}
L5	Adult male	1.16×10^{-1}	6.49×10^{-4}	1.17×10^{-1}
	Adult female	0.97×10^{-1}	5.05×10^{-4}	0.98×10^{-1}
L6	Adult male	0.93×10^{-1}	5.21×10^{-4}	0.94×10^{-1}
	Adult female	0.78×10^{-1}	4.06×10^{-4}	0.78×10^{-1}
Average	Adult male	1.25×10^{-1}	6.97×10^{-4}	1.26×10^{-1}
	Adult female	1.04×10^{-1}	5.43×10^{-4}	1.05×10^{-1}

Table 8 | Annual committed equivalent and effective doses of radon in tap water to adult resident gastrointestinal tracts

Sample code	Annual committed equivalent doses of ^{222}Rn (μSv a^{-1}) Stomach	Small intestine	Upper large intestine	Lower large intestine	Annual committed effective dose (μSv a^{-1})
L1	0.1842	0.1513	1.2217	1.5514	0.1900
L2	0.1991	0.1636	1.3208	1.6772	0.2054
L3	0.2638	0.2167	1.7500	2.2223	0.2722
L4	0.2041	0.1676	1.3538	1.7191	0.2105
L5	0.1394	0.1145	0.9245	1.1740	0.1438
L6	0.0498	0.0409	0.3302	0.4193	0.0514
Average	0.1734	0.1424	1.1502	1.4606	0.1789

effective contribution of sample group L2 to residents was the highest, and that of adult male and an adult female was 0.152 and 0.127 μSv a^{-1}, respectively, and the annual committed effective dose of sample group L6 was the lowest, 0.094 and 0.078 μSv a^{-1}, respectively, which were all lower than the upper reference value of about 10 mSv a^{-1} set by ICRP (ICRP 2014).

Table 8 shows the annual committed effective dose and annual committed equivalent dose caused by ^{222}Rn in tap water entering the residents' gastrointestinal tract. The annual committed effective dose of sample group L3 is the highest, and that of sample group L6 is the lowest, which is 0.2722 and 0.0514 μSv a^{-1}, respectively. Among all the regions of the gastrointestinal tract, the lower large intestine region had the highest average annual committed equivalent dose (1.4606 μSv a^{-1}), followed by the upper large intestine region (1.1502 μSv a^{-1}), and the small intestine region was the lowest (0.1424 μSv a^{-1}).

4. CONCLUSION

In this study, the radon concentration in the tap water of six residential areas was measured, and the average radon concentration was 548.16 mBq L^{-1}. All samples were under the radon concentration limits recommended by USEPA and EURATOM (11.11 Bq L^{-1} and 100 Bq L^{-1}). Compared with the radon concentration in the tap water of other countries or regions, the radon concentration in this study is within the range of other measurement results. At the same time, the radon concentration and the retention rate under different temperatures were obtained by heating tap water in the water bath, and the radon concentration generally showed a downward trend with the increase in temperature. Finally, the dose calculation model provided by ICRP was used to estimate the dose of radon exposure in some water-use scenarios. In the process of the shower, the annual committed effective dose of radon progenies to the male respiratory tract and the alimentary tract is higher than that of female, and in the respiratory tract, the committed equivalent dose caused by α activities to the respiratory tract target tissue is higher than that of β activities, while the average annual committed effective dose of radon from drinking water ingestion to the resident gastrointestinal tract is 0.1789 μSv a^{-1}. Urban water supply plants, therefore, can reduce the concentration of radon in the water source by centralized aeration, while residents can reduce the concentration of radon in the water by heating and degassing to avoid further increase of public exposure to radon.

ACKNOWLEDGEMENTS

The work is supported by the National Natural Science Foundation of China (Project No. 32060292). The authors are thankful to the Xinjiang Hongfu Nuclear Safety Technology Co., Ltd of China for providing facilities and support.

DATA AVAILABILITY STATEMENT

All relevant data are included in the paper or its Supplementary Information.

REFERENCES

Ahmad, N., Jaafar, M. S. & Alsaffar, M. S. 2015 Study of radon concentration and toxic elements in drinking and irrigated water and its implications in Sungai Petani, Kedah, Malaysia. *J. Radiat. Res. Appl. Sci.* **8** (3), 294–299.

Alghamdi, A. S. & Aleissa, K. A. 2014 Influences on indoor radon concentrations in Riyadh, Saudi Arabia. *Radiat. Meas.* **62**, 35–40.

Binesh, A., Mowlavi, A. A. & Mohammadi, S. 2012 Estimation of the effective dose from radon ingestion and inhalation in drinking water sources of Mashhad, Iran. *Iran. J. Radiat. Res.* **10** (1), 37–41.

Council Directive 2013/51/Euratom. 2013 Laying down requirements for the protection of the health of the general public with regard to radioactive substances in water intended for human consumption. *Off. J. Eur. Union L.* **296/12**, 12–21.

Darby, S., Hill, D., Auvinen, A., Barros-Dios, J. M., Baysson, H., Bochicchio, F., Deo, H., Falk, R., Forastiere, F., Hakama, M., Heid, I., Kreienbrock, L., Kreuzer, M., Lagarde, F., Mäkeläinen, I., Muirhead, C., Oberaigner, W., Pershagen, G., Ruano-Ravina, A., Ruosteenoja, E., Schaffrath Rosario, A., Tirmarche, M., Tomášek, L., Whitley, E., Wichmann, H. E. & Doll, R. 2005 Radon in homes and risk of lung cancer: collaborative analysis of individual data from 13 European case-control studies. *Br. Med. J.* **330** (7485), 223–226.

Erdogan, M., Manisa, K. & Tel, F. 2015 The measurement of radon activity concentrations in tap water in some dwellings of Konya province-Turkey. *Carpathian J. Earth Environ. Sci.* **10** (1), 273–278.

Fakhri, Y., Kargosha, M., Langarizadeh, G., Zandsalimi, Y., Rasouli Amirhajeloo, L., Moradi, M., Moradi, B. & Mirzaei, M. 2015 Effective dose Radon 222 of the tap water in children and adults people; Minab City, Iran. *Global J. Health Sci.* **8** (4), 234–243.

ICRP (International Commission on Radiological Protection) 1979 *Limits for Intakes of Radionuclides by Workers*. Pergamon Press, Oxford. ICRP Publication 30, Part 1. Annals of the ICRP.

ICRP (International Commission on Radiological Protection) 1994 *Human Respiratory Tract Model for Radiological Protection*. Pergamon Press, Oxford. ICRP Publication 66, Annals of the ICRP.

ICRP (International Commission on Radiological Protection) 2002a *Guide for the Practical Application of the ICRP Human Respiratory Tract Model*. Pergamon Press, Oxford. ICRP Supporting Guidance 3, Annals of the ICRP.

ICRP (International Commission on Radiological Protection) 2002b *Basic Anatomical and Physiological Data for Use in Radiological Protection: Reference Values*. Pergamon Press, Oxford. ICRP Publication 89, Annals of the ICRP.

ICRP (International Commission on Radiological Protection) 2007 *Nuclear Decay Data for Dosimetric Calculations*. Pergamon Press, Oxford. ICRP Publication 107, Annals of the ICRP.

ICRP (International Commission on Radiological Protection) 2014 *Radiological Protection Against Radon Exposure*. Pergamon Press, Oxford. ICRP Publication 126, Annals of the ICRP.

ICRP (International Commission on Radiological Protection) 2015 *Occupational Intakes of Radionuclides: Part 1*. Pergamon Press, Oxford. ICRP Publication 130, Annals of the ICRP.

ICRP (International Commission on Radiological Protection) 2016 *The ICRP Computational Framework for Internal Dose Assessment for Reference Adults: Specific Absorbed Fractions*. Pergamon Press, Oxford. ICRP Publication 133, Annals of the ICRP.

Jantsikene, A., Kiisk, M., Suursoo, S., Koch, R. & Lumiste, L. 2014 Groundwater treatment as a source of indoor radon. *Appl. Radiat. Isot.* **93**, 70–75.

Kendall, G. M. & Smith, T. J. 2002 Doses to organs and tissues from radon and its decay products. *J. Radiol. Prot.* **22**, 389–406.

Kulali, F., Günay, O. & Aközcan, S. 2019 Determination of indoor radon levels at campuses of Üsküdar and Okan Universities. *Int. J. Environ. Sci. Technol.* **16** (9), 5281–5284.

Le, C. H., Huynh, N. P. T., Nguyen, V. T. & Le, Q. B. 2015 Radon and radium concentrations in drinkable water supplies of the Thu Duc region in Ho Chi Minh City, Vietnam. *Appl. Radiat. Isot.* **105**, 219–224.

Marques, A. L., Dos Santos, W. & Geraldo, L. P. 2004 Direct measurements of radon activity in water from various natural sources using nuclear track detectors. *Appl. Radiat. Isot.* **60** (6), 801–804.

Mehra, R., Kaur, K. & Bangotra, P. 2016 Annual effective dose of radon due to exposure in indoor air and groundwater in Bathinda district of Punjab. *Indoor Built Environ.* **25** (5), 848–856.

Misdaq, M. A. & Flata, K. 2003 Radon and daughters in cigarette smoke measured with SSNTD and corresponding committed equivalent dose to respiratory tract. *Radiat. Meas.* **37** (1), 31–38.

Misdaq, M. A., Ghilane, M., Ouguidi, J. & Outeqablit, K. 2012 Radiation doses to individuals due to ^{238}U, ^{232}Th and ^{222}Rn from the immersion in thermal waters and to radon progeny from the inhalation of air inside thermal stations. *Radiat. Environ. Biophys.* **51** (4), 375–389.

Nazaroff, W. W., Doyle, S. M., Nero, A. V. & Sextro, R. G. 1987 Potable water as a source of airborne ^{222}Rn in U.S. Dwellings: a review and assessment. *Health Phys.* **52** (3), 281–295.

Nita, D. C., Moldovan, M., Sferle, T., Ona, V. D. & Burghele, B. D. 2013 Radon concentrations in water and indoor air in North-West regions of Romania. *Rom. Rep. Phys.* **58** (Supplement), 196–201.

Oner, F., Yalim, H. A., Akkurt, A., Orbay, M. & Faculty, A. 2009 The measurements of radon concentrations in drinking water and the Yeşilirmak River water in the area of Amasya in Turkey. *Radiat. Prot. Dosim.* **133** (4), 223–226.

Pagava, S., Rusetski, V., Robakidze, Z., Farfán, E. B., Dunker, R. E., Popp, J. L., Avtandilashvili, M., Wells, D. P. & Donnelly, E. H. 2008 Initial investigation of ^{222}Rn in the Tbilisi urban environment. *Health Phys.* **95** (6), 761–765.

Planinić, J., Radolić, V., Faj, Z. & Šuveljak, B. 1997 Radon equilibrium factor and aerosols. *Nucl. Instrum. Methods Phys. Res., Sect. A* **396** (3), 414–417.

Rusconi, R., Forte, M., Badalamenti, P., Bellinzona, S., Gallini, R., Maltese, S., Romeo, C. & Sgorbati, G. 2004 The monitoring of tap waters in Milano: planning, methods and results. *Radiat. Prot. Dosim.* **111** (4), 373–376.

Sarrou, I. & Pashalidis, I. 2003 Radon levels in Cyprus. *J. Environ. Radioact.* **68** (3), 269–277.

Sharma, S., Kumar, A., Mehra, R. & Kaur, R. 2019 Ingestion and inhalation doses due to intake of radon in drinking water samples of Amritsar province, Punjab, India. *Radiat. Prot. Dosim.* **187** (2), 230–242.

UNSCEAR (United Nations Scientific Committee on the Effects of Atomic Radiation) 2000 *Sources and Biological Effects of Ionizing Radiation*. UNSCEAR Report to the General Assembly, New York, United Nations.

USEPA (United States Environmental Protection Agency) 1999 *Technical Factsheet: Proposed Radon in Drinking Water Rule*. USEPA, Washington, DC.

Vinson, D. S., Campbell, T. R. & Vengosh, A. 2008 Radon transfer from groundwater used in showers to indoor air. *Appl. Geochem.* **23** (9), 2676–2685.

WHO (World Health Organization) 2009 *Guidelines for Drinking-water Quality*. WHO Press, Geneva.

Yasouka, Y., Ishikawa, T., Tokonami, S., Takahashi, H., Narazaki, Y. & Sinogi, M. 2008 A case study on the effect of water from groundwater sources on indoor radon levels. *J. Radioanal. Nucl. Chem.* **275** (1), 165–172.

Yong, J. L., Feng, G. W., Liu, Q., Tang, C., Wu, B. S., Hu, Y. H., Cai, C. L. & Mao, P. H. 2020 Radon concentration measurement and effective dose assessment in different brands of commercial bottled water produced in China. *Water Suppl.* **20** (5), 1581–1591.

Zhuo, W., Iida, T. & Yang, X. 2001 Occurrence of ^{222}Rn, ^{226}Ra, ^{228}Ra and U in groundwater in Fujian Province, China. *J. Environ. Radioact.* **53** (1), 111–120.

First received 30 April 2021; accepted in revised form 23 October 2021. Available online 9 November 2021